

B. 研究内容と成果

B-1. W鍍デバイス用Si製鍍ベースの製作

Wの鍍を立てて固定し、配線を取り出すベース部分をSiウエハを使ったリソグラフ技術とエッチング及び成膜技術により作成した。表1にプロセスフローを示す。

表1 Si製鍍ベース部材製作プロセス

大工程	断面図	プロセス	使用装置
1 Siウエハ熱酸化		(100)高抵抗(1kΩcm) 4インチ, 0.525mmt スチーム酸化(1100℃)	酸化炉
2 リソグラフ(段差形成)		酸化膜ハターニング BHF処理	ウエットエッチング器具
3 異方性ウエットエッチング		THAH処理 (アルカリエッチング)	アルカリエッチング処理装置
4 リソグラフ(貫通孔形成)		表面酸化膜ハターニング BHF処理	ウエットエッチング器具
5 異方性ドライエッチング		DRIE処理 (Deep Reactive Ion Etching)	DRIE装置
6 再熱酸化		スチーム酸化 (1100℃) 1.5μm	酸化炉
7 リソグラフ(メタライズ)			
8 メタルスパッタ		Au/Pt/Ti (300/25/50nm)	3元スパッタ装置
9 メタライズ		リフトオフ	
10 洗浄・小片化		カッティング	ダイシング装置

チップ寸法	チップ実物写真 (表・裏)
<p>200 × 400, 孔100 μm □ 150 × 300, 孔70 μm φ Au/Pt/Ti/SiO₂/Siベース Auリード線固定用孔 W鍍挿入用孔 525</p>	

B-2. W鍼の製作

<線材の先鋭化の原理>

W鍼は、50 μm ϕ の線材を用い、電解エッチングによって先端を針状に尖らせた。図1に、電解エッチング法の原理とW線のエッチング例を示す。

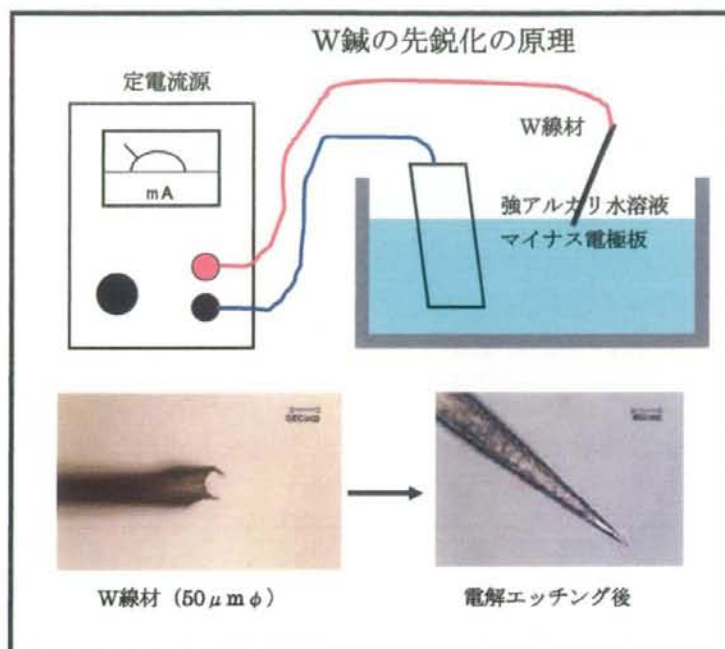


図1 電解エッチング法によるW鍼形成

Wの電解エッチング液は、KOH水溶液(40wt%)を用いた。電極板は導通が取れてアルカリに強い金属であれば良い。今回はCrめっきされた薄い鉄板を使用した。

W線に定電流源のプラス極からリード線をワニロクリップなどで接続し、マイナス電極板の入ったKOH水溶液に先端2mm程度を投入し通電する。WはKOH水溶液中にWイオンとして溶解し、先端から細くなり、最終的に図1右下の写真のように先鋭化される。反応中は泡が発生する。水溶液から取り出す目安は先端が尖ってくると電圧表示が急に高くなるのでその時点で取り出すとほぼ同じ形状の針が得られる。

<有機コーティング(バリレンコート)>

W鍍に絶縁膜を形成する。絶縁膜は、撥水性、耐薬品性にも優れて安定な有機膜として医療器具分野、電子回路分野などに広く使われているポリパラキシレン(バリレン)樹脂を使用した(アウトソースにて製作)。これはCVD(Chemical Vapor Deposition)によるので、分子レベルでのコンフォーマルな膜付けが可能である。プロセスは以下の通りである。

- 原料ダルマー(粉末・パラキシリレン2量体)を気化室に入れて加熱する。
- 加熱蒸発したダルマーは、高温の熱分解室に導かれて、ここで反応性の高いラジカルなモノマー(パラキシリレン)になる。
- ラジカル化した蒸気が蒸着室内で物体に接し、そこで重合して高分子膜(バリレン樹脂膜)を生成する。

図2に、W鍍に $5\mu\text{m}$ 厚でCVDしたバリレン膜を鍍先端のみ被覆除去した状態の写真を示す。



図2 バリレンコートW線(先端部リリース)

<鍍デバイス>

鍍デバイスは、Si台座の中央部にバリレンコートW鍍(W線 $50\mu\text{m}\phi$ 、バリレン $5\mu\text{m}$ 厚)を挿入固定した鍍部と、同じくSi台座にウレタンコートAu線(Au線 $60\mu\text{m}\phi$ 、ウレタン $7.5\mu\text{m}$ 厚)を導通接続した導線部(約 15cm)と電極端子(差動アンプとの接続端子)を主な構成部材としている。図3にデバイス全体の写真を示す。

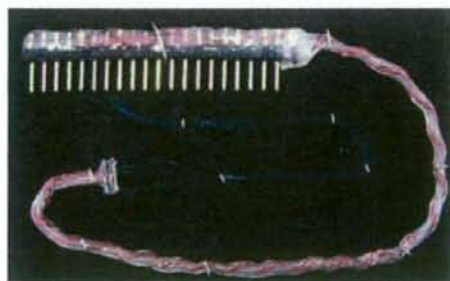


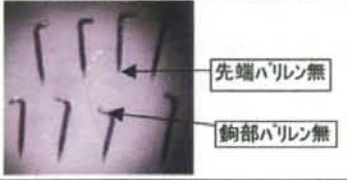
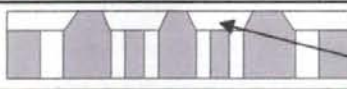
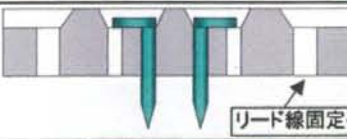

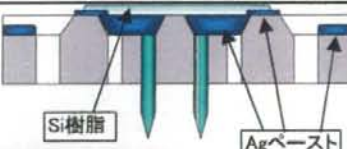

図3

鍍デバイス組立てプロセスは、下記のようなものである。

組立てプロセス（1） W鍍のSiベースへの取り付け(表3-1)

W鍍は、Si台座表面から、0.25~0.4mm程度突き出るように長さを調整した。またSiベースの鍍受け部にパリエレン被覆を除去して根元を90度折り曲げて、Siベースに固定・接着できるようにした。鍍受け部にAgペーストを満たし、~150℃で数分間乾燥・固化により、鍍と後のリード線への電氣的導通経路を保ちつつしっかり固定する。

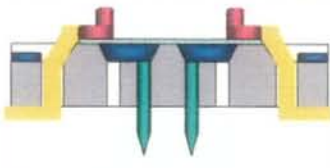

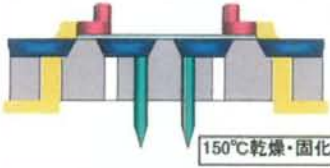

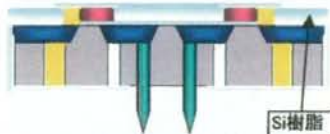

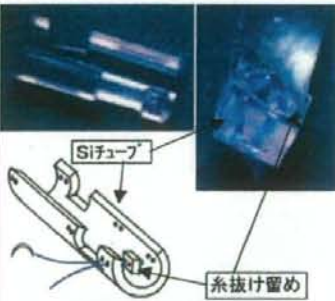



表 3-1 W線鍍形成と Si ベースへの取り付け

大工程	断面鳥瞰図・写真	プロセス・写真
1 W鍍の形成		<p>鍍先端のパリエレンコート を除去し、先端から650 μm ~800 μmの長さで曲げ 曲げたところを150 μm 程度残してカットし、パリエレン も除去する。</p>
2 Si台座アッセンブリ		<p>Si台座断面 鍍受け部</p>
①鍍挿入		
②Agペースト充填 乾燥・硬化 ③硬化後 樹脂被覆	 	<p>Agペーストで完全に埋込み 150℃乾燥・固化</p>

組立てプロセス（2） Au配線の接続と伸縮機構の製作(表3-2)

ウレタン被覆を約2mm程度除去したAu線を、Siベースの両端に形成したリード線固定孔へ挿入し、孔に巻きつけて仮固定する(⑤)。次にAgペーストでAu線のあるパッド部全体を満たし、固化させる。乾燥後、Agペーストによる電気的リークがないことを確認し、余分なAu線を取り除き、Si樹脂をSi台座全体に塗布して絶縁を兼ねた保護を兼ねた処理を施す(⑦)。

表 3-2 リード線の処理と神経固定用チューブの取り付け

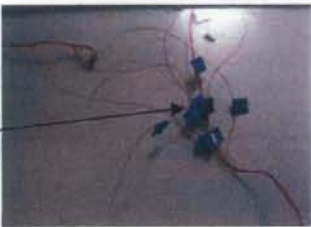



⑤Au線挿入巻付け		
⑥Agペースト注入	 <p>150°C乾燥・固化</p>	
⑦Au線調整・樹脂被覆	 <p>Si樹脂</p>	
3 神経固定器具形成 ①Siチューブに ナイロン糸取り付け	 <p>Siチューブ</p> <p>糸抜け留め</p>	<p>Siチューブ(1.5×2.5mmφ)の上部を90°切り取る。台座固定部分を切り取る。約40μm厚の糸抜け留めを通しナイロン糸を6箇所に取り付ける。</p> 
②Siチューブと一体化	 <p>Siチューブ鍼デバイス本体をSi樹脂で固定</p>	 <p>チューブ横から見た状態</p>

次に、図3-2 3-①に示すように、神経固定用のSiチューブを準備し、上部90度を切り取る。鍼デバイス固定部分を切り抜き、手術糸プロロン6-0に糸抜け留めを通しチューブ6箇所10cmの長さで取り付ける。最後に鍼デバイスをSiチューブへ挿入・接着固定する。

組立てプロセス (3) 電極分岐端子の接続と固定 (表3-3, 3-4)


Auワイヤーは、10本のW鍍と電氣的にそれぞれ独立接続される必要があるため、電極端子のNo.と鍍の関係が明確である必要がある。このため、Au線1本1本にNo札をつけ、電極端子に順番に接続される。また10本のAu線に伸縮性をもたせるために、Siチューブに螺旋状に巻き付け固定した。Siチューブは、鍍デバイス部のSiチューブと電極端子にしっかり接着固定される。詳細手順は表3-3及び3-4を参照。

表3-3 Auワイヤー処理その1

<p>4 Auワイヤー処理</p> <p>①鍍とNo.が一致するようにAu線に番号札をつける</p> <p>1~20まで1枚ずつNo.が振ってある</p>		<table border="1"> <thead> <tr> <th colspan="2">鍍No.</th> </tr> </thead> <tbody> <tr> <td>1</td> <td>6</td> </tr> <tr> <td>2</td> <td>7</td> </tr> <tr> <td>3</td> <td>8</td> </tr> <tr> <td>4</td> <td>9</td> </tr> <tr> <td>5</td> <td>10</td> </tr> </tbody> </table>	鍍No.		1	6	2	7	3	8	4	9	5	10
鍍No.														
1	6													
2	7													
3	8													
4	9													
5	10													
<p>②Auワイヤーを束ねて振り合わせ1束のリード線とし、Si樹脂を塗って保護する。更に外径1mmφ程度のSiチューブを少し伸ばした状態で固定し、これにリード線の束を巻きつけ、Si接着材で固定する。固まったら伸ばしていたSiチューブを開放する。リード部は伸縮可能なリード線になっている。リード線は、真直ぐな状態で280mm、Siチューブに巻き付けた状態で140~150mm程度になる。30~40mmはSiチューブごと引き伸ばせる構造になっている。</p> 														
<p>③鍍デバイス部とSiチューブを、エポキシ樹脂及びSi接着剤により固着する。</p> 														
<p>④Au端子と電極端子との接続 ※引き出し電極端子として用いたIC電極端子</p> <p>22ピンタイプ</p>														

マウントベース治具に対し、Au線の末端を表3-4に示す手順で接続して行く。基本的にAgペーストで導通を取り、固定する方法は変わらない。最後にAu線を巻き付けているSiチューブとマウントベースを接着固定し、完成となる。

表3-4 Auワイヤー処理その2

<p>(配線接続ターミナル)</p> <p>④-1 Au線の巻き付け</p>		<p>短い端子側にAu線を巻き付ける Agペーストで固定</p>
<p>④-2 配線固定・まとめ</p>		<p>Siチューブを電極端子へ接着</p>
<p>④-3 電極端子固定一体化</p>		<p>余ったリード線の束をまとめて Siチューブへ巻き付けしっかり 接着・固定</p>
<p>(完成例)</p> 		

<倫理面への配慮>

本研究の動物実験は、国立循環器病センター研究所および日本生理学学会の動物実験の指針に沿い、実験動物の数と侵襲を最小にするよう、また、動物愛護上においても、十分配慮して行われた。また、国立循環器病センター研究所実験動物委員会に承認のもとに、行われた。

D. 健康危険情報

健康危険情報は特になし。

E. 研究発表

1. 論文発表

Kawada T, Shimizu S, Yamamoto H, Shishido T, Kamiya A, Miyamoto T, Sunagawa K, Sugimachi M. Servo-Controlled Hind-Limb Electrical Stimulation for Short-Term Arterial Pressure Control. *Circ J* 2008 (in press)

Yamamoto H, Kawada T, Kamiya A, Kita T, Sugimachi M. Electroacupuncture changes the relationship between cardiac and renal sympathetic nerve activities in anesthetized cats. *Auton Neurosci*. 2008 Dec 15;144(1-2):43-9. PMID: 18990613

Mizuno M, Kamiya A, Kawada T, Miyamoto T, Shimizu S, Shishido T, Sugimachi M. Accentuated antagonism in vagal heart rate control mediated through muscarinic potassium channels. *J Physiol Sci*. 2008 Dec;58(6):381-8. PMID: 18842163

Miyamoto T, Kawada T, Yanagiya Y, Akiyama T,

Kamiya A, Mizuno M, Takaki H, Sunagawa K, Sugimachi M. Contrasting effects of intrinsic operation and extrinsic activation of presynaptic α_2 -adrenergic inhibition on sympathetic heart rate control. *Am J Physiol Heart Circ Physiol*. 2008 Nov;295(5):H1855-66. PMID: 18757478

Yamamoto K, Kawada T, Kamiya A, Takaki H, Shishido T, Sunagawa K, Sugimachi M. Muscle mechanoreflex augments arterial baroreflex-mediated dynamic sympathetic response to carotid sinus pressure. *Am J Physiol Heart Circ Physiol*. 2008 Sep;295(3):H1081-H1089. PMID: 18586892

Kamiya A, Kawada T, Yamamoto K, Mizuno M, Shimizu S, Sugimachi M. Upright tilt resets dynamic transfer function of baroreflex neural arc to minimize the pressure disturbance in total baroreflex control. *J Physiol Sci*. 2008 Jun;58(3):189-98. PMID: 18471343

Kamiya A, Michikami D, Iwase S, Mano T. Decoding rule from vasoconstrictor skin sympathetic nerve activity to nonglabrous skin blood flow in humans at normothermic rest. *Neurosci Lett*. 2008 Jul 4;439(1):13-7. PMID: 18502048

2. 学会発表

M. Mizuno, A. Kamiya, T. Kawada and M. Sugimachi. Muscarinic potassium channels play a significant role in the negative chronotropic response with or without background sympathetic tone. EXPERIMENTAL

神谷 厚範、杉町 勝 自律神経活動をモニター且つ刺激するマルチ電極MEMS神経装置の開発 第47回日本生体医工学会大会

水野 正樹、神谷 厚範、川田 徹、穴戸 稔聡、杉町 勝 交感神経緊張はムスカリンK+チャンネルによる徐脈作用の迅速性に影響を及ぼさない 第47回日本生体医工学会大会

清水 秀二、穴戸 稔聡、川田 徹、水野 正樹、日高 一郎、上村 和紀、神谷 厚範、杉町 勝 Ebstein奇形における右房化右室が2心室修復術後の心機能に与える影響 第47回日本生体医工学会大会

川田 徹、清水 秀二、水野 正樹、神谷 厚範、穴戸 稔聡、杉町 勝 血圧制御のための電気鍼の刺激強度調節システムの開発 第47回日本生体医工学会大会

M.Sugimachi, T.Kawada, H.Yamamoto, A.Kamiya, T.Miyamoto, K.Sunagawa
Modification of Autonomic Balance by Electrical Acupuncture Does Not Affect Baroreflex Dynamic Characteristics 30th Annual International Conference of the IEEE Engineering in Medicine and Biology Society

M.Sugimachi, K.Uemura, T.Shishido, A.Kamiya, S.Shimizu, K.Sunagawa Theoretical and experimental demonstration of minimizing O₂ consumption under preserved hemodynamics in heart failure XVIII th Cardiovascular System

水野 正樹、川田 徹、神谷 厚範、穴戸 稔聡、杉町 勝. ラット交感および迷走神経刺激に対する動的心拍数応答. 第101回近畿生理学談話会

清水 秀二、秋山 剛、川田 徹、水野 正樹、神谷 厚範、穴戸 稔聡、杉町 勝. 心臓マイクログアイアリス法による心房アセチルコリン濃度の定量化. 第101回近畿生理学談話会

3. マスコミなどへの発表
なし

F. 知的財産権の出願・登録状況

4. 特許取得

【発明の名称】神経信号用プローバ、神経信号出力装置、神経信号記録装置、神経刺激装置及び神経信号入出力装置

【名称】神経信号用プローバ、神経信号出力装置、神経信号記録装置、神経刺激装置及び神経信号入出力装置

【発明者】神谷厚範、杉町 勝、桜井史敏、慶光院利映

【出願日】平成 19 年 2 月 1 日

【出願番号】特願 2007-023501

5. 実用新案登録

なし。

6. その他

なし

研究成果の刊行に関する一覧表

書籍
なし

雑誌

発表者氏名	論文タイトル名	発表誌名	巻号	ページ	出版年
Kawada T, Shimizu S, Yamamoto H, Shishido T, Kamiya A, Miyamoto T, Sunagawa K, Sugimachi M.	Servo-Controlled Hind-Limb Electrical Stimulation for Short-Term Arterial Pressure Control.	Circ J			in press
Yamamoto H, Kawada T, Kamiya A, Kita T, Sugimachi M.	Electroacupuncture changes the relationship between cardiac and renal sympathetic nerve activities in anesthetized cats.	Auton Neurosci	144	43-49	2008
Mizuno M, Kamiya A, Kawada T, Miyamoto T, Shimizu S, Shishido T, Sugimachi M.	Accentuated Antagonism in Vagal Heart Rate Control Mediated through Muscarinic Potassium Channels.	J Physiol Sci	58	381-388	2008
Miyamoto T, Kawada T, Yanagiya Y, Akiyama T, Kamiya A, Mizuno M, Takaki H, Sunagawa K, Sugimachi M.	Contrasting effects of presynaptic alpha2-adrenergic autoinhibition and pharmacologic augmentation of presynaptic inhibition on sympathetic heart rate control.	Am J Physiol Heart Circ Physiol	295	H1855-1866	2008
Yamamoto K, Kawada T, Kamiya A, Takaki H, Shishido T, Sunagawa K, Sugimachi M.	Muscle mechanoreflex augments arterial baroreflex-mediated dynamic sympathetic response to carotid sinus pressure.	Am J Physiol Heart Circ Physiol	295	H1081-H1089	2008
Kamiya A, Kawada T, Yamamoto K, Mizuno M, Shimizu S, Sugimachi M.	Upright tilt resets dynamic transfer function of baroreflex neural arc to minimize the pressure disturbance in total baroreflex control.	J Physiol Sci	58	189-198	2008
Kamiya A, Michikami D, Iwase S, Mano T.	Decoding rule from vasoconstrictor skin sympathetic nerve activity to nonglabrous skin blood flow in humans at normothermic rest.	Neurosci Lett.	Jul 4; 439(1)	13-7	2008



Contents lists available at ScienceDirect

Autonomic Neuroscience: Basic and Clinical

journal homepage: www.elsevier.com/locate/autneu



Electroacupuncture changes the relationship between cardiac and renal sympathetic nerve activities in anesthetized cats

Hiromi Yamamoto ^{a,*}, Toru Kawada ^b, Atsunori Kamiya ^b, Toru Kita ^a, Masaru Sugimachi ^b

^a Department of Cardiovascular Medicine, Graduate School of Medicine, Kyoto University, Kyoto 606-8501, Japan

^b Department of Cardiovascular Dynamics, Advanced Medical Engineering Center, National Cardiovascular Center Research Institute, Osaka 565-8565, Japan



Electroacupuncture changes the relationship between cardiac and renal sympathetic nerve activities in anesthetized cats

Hiromi Yamamoto^{a,*}, Toru Kawada^b, Atsunori Kamiya^b, Toru Kita^a, Masaru Sugimachi^b

^a Department of Cardiovascular Medicine, Graduate School of Medicine, Kyoto University, Kyoto 606-8501, Japan

^b Department of Cardiovascular Dynamics, Advanced Medical Engineering Center, National Cardiovascular Center Research Institute, Osaka 565-8565, Japan

ARTICLE INFO

Article history:

Received 5 June 2008

Received in revised form 13 August 2008

Accepted 12 September 2008

Keywords:

Hind limb stimulation
Baroreflex
Arterial blood pressure
Heart rate

ABSTRACT

Electroacupuncture (EA) is known to affect hemodynamics through modulation of efferent sympathetic nerve activity (SNA), however, possible regional differences in the SNA response to EA remains to be examined. Based on the discordance between arterial blood pressure and heart rate changes during EA, we hypothesized that regional differences would occur among SNAs during EA. To test this hypothesis, we compared changes in cardiac and renal SNAs in response to 1-min EA (10 Hz or 2 Hz) of a hind limb in adult cats anesthetized with pentobarbital sodium. Renal SNA remained decreased for 1 min during EA ($P < 0.01$ for both 10 Hz and 2 Hz). In contrast, cardiac SNA tended to decrease only in the beginning of EA. It increased during the end of EA ($P < 0.05$ for 2 Hz) and further increased after the end of EA ($P < 0.01$ both for 10 Hz and 2 Hz). There was a quasi-linear relationship between renal and cardiac SNAs with a slope of 0.69 (i.e., renal SNA was more suppressed than cardiac SNA) during the last 10 s of EA. The discrepancy between the renal and cardiac SNAs persisted after sinoaortic denervation and vagotomy. In conclusion, EA evokes differential patterns of SNA responses and changes the relationship between cardiac and renal SNAs.

© 2008 Elsevier B.V. All rights reserved.

1. Introduction

Electroacupuncture stimulation has been used to modulate autonomic nervous activity and cardiovascular function (Kimura and Sato, 1997; Lin et al., 2001). Several studies have demonstrated that arterial blood pressure (AP) is decreased by acupuncture-like stimulation in anesthetized animals (Kline et al., 1978; Ku and Zou, 1993; Lee and Kim, 1994; Zhou et al., 2005). The cardiovascular responses induced by acupuncture-like stimulation are reflexes mediated via somatic afferent nerves and autonomic efferent nerves (Sato et al., 1994, 2002). Although slow-onset, long-lasting effects may be characteristics of acupuncture, rapid-onset, short-lasting effects are also reported in some experimental conditions. In anesthetized rats, Ohsawa et al. (1995) reported that acupuncture-like stimulation of a hind limb decreased AP in association with a decrease in renal sympathetic nerve activity (RSNA). Uchida et al. (2007) reported that acupuncture-like stimulation of a hind limb induced decreases in cardiac sympathetic nerve activity (CSNA) and heart rate (HR). On the other hand, Kobayashi et al. (1998) reported that acupuncture stimulation produced variable responses including tachycardia, bradycardia, or no responses. We hypothesized that regional differences in sympathetic nerve activities would account for the diverse HR response and more consistent hypotensive response reported during EA. Although Sato et al. (1981) reported that stimulation of group III muscle afferent fibers of a hind limb induces either bradycardic or tachycardic response in anesthetized cats, they did

not measure efferent sympathetic nerve activities. To test the hypothesis that EA would evoke regional differences among sympathetic efferent nerve activities, we simultaneously recorded and directly compared CSNA and RSNA during EA in anesthetized cats. The kidneys are important for a long-term AP control via the maintenance of sodium and water balance (DiBona, 2005). At the same time, because the kidneys receive approximately 20% of the cardiac output in resting humans (Rowell, 1974), we thought changes in RSNA could contribute to the acute AP control. We first examined changes in AP, HR, CSNA, and RSNA in response to 10-Hz or 2-Hz EA of a hind limb. We then investigated possible roles of arterial baroreflex and vagal nerve activities in the effects of EA using sinoaortic denervation and vagotomy.

2. Methods

2.1. Surgical preparation

Animal care was provided in strict accordance with the Guiding Principles for the Care and Use of Animals in the Field of Physiological Sciences approved by the Physiological Society of Japan. All protocols were approved by the Animal Subject Committee of National Cardiovascular Center. Adult cats weighing 3.0 to 5.2 kg were anesthetized by an intraperitoneal injection of pentobarbital sodium (30–35 mg/kg) and ventilated mechanically via a tracheal tube with oxygen-supplied room air. The depth of anesthesia was maintained with a continuous intravenous infusion of pentobarbital sodium ($1\text{--}2\text{ mg}\cdot\text{kg}^{-1}\cdot\text{h}^{-1}$) through a catheter inserted into the right femoral vein. Vecuronium bromide (0.5–

* Corresponding author. Tel.: +81 75 751 3195; fax: +81 75 751 3203.
E-mail address: hiromi@kuhp.kyoto-u.ac.jp (H. Yamamoto).

1.0 mg·kg⁻¹·h⁻¹, i.v.) was given continuously to suppress muscular activity. AP was measured using a catheter-tip manometer inserted from the right femoral artery and advanced into the thoracic aorta. A pair of bipolar stainless steel wire electrodes (AS633, Cooner Wire, Chatsworth, CA) was attached to a branch of the left renal nerve through a flank incision. The nerve fibers peripheral to the electrodes were tightly ligated and crushed to remove afferent signals from the kidney. The nerve fibers and the electrodes were secured with silicone glue (Kwik-Sil, World Precision Instruments, Sarasota, FL). Another pair of bipolar stainless steel wire electrodes was attached to a branch of the left cardiac sympathetic nerve arising from the left stellate ganglion through a resection of the left second rib. The nerve fibers distal to the electrodes were sectioned to eliminate afferent signals from the heart. The nerve fibers and the electrodes were secured with silicone glue. Because the influence of the right cardiac sympathetic nerve on sinus rhythm is greater than that of the left cardiac sympathetic nerve (Yasunaga and Nosaka, 1979), we kept the right cardiac sympathetic nerve intact to preserve the HR response to EA. One rationale for recording left CSNA was that there was no significant laterality in left and right CSNAs during sympathetic perturbation via the arterial baroreflex (Kawada et al., 2003). The preamplified nerve activity signals were band-pass-filtered between 150 and 1000 Hz and then rectified and low-pass-filtered with a cut-off frequency of 30 Hz to quantify CSNA and RSNA. For sinoaortic denervation and vagotomy, we sectioned all nerves surrounding the common carotid arteries at the neck. The carotid sinus nerves were crushed by tight ligatures of 3–0 silk suture around tissues between the internal and external carotid arteries.

2.2. Electroacupuncture

In the supine position, both hind limbs were lifted to obtain a better view of the lateral sides of the lower legs. An EA needle with a

diameter of 0.2 mm (CE0123, Seirin-Kasei, Japan) was inserted into a point below the knee joint just lateral to the tibia to the depth of approximately 10 mm. Another EA needle was inserted into the skin behind the ankle as the ground. EA was applied to either the left or right leg using an isolator connected to an electrical stimulator (SEN 7203, Nihon Kohden, Japan). The pulse width was set at 500 μ s and the stimulus frequency was set at either 10 or 2 Hz. The stimulus current was set in the range from 2 to 5 mA (2.9 \pm 1.1 mA, mean \pm SD) to produce an AP decrease of more than 5 mmHg at 10-Hz stimulation.

2.3. Protocols

Protocol 1. To examine regional differences in sympathetic nerve activities, we applied 10-Hz or 2-Hz EA for 1 min while measuring AP, HR, CSNA, and RSNA. EA was applied to either the left or right hind limb in random order. An interval of at least 5 min was allowed between the EA trials.

Protocol 2. We applied 10-Hz electrical stimulation to a nonspecific control point in the front of the right thigh to examine whether changes in AP, HR, CSNA, and RSNA observed in Protocol 1 were caused by nonspecific responses to the electrical stimulation.

Protocol 3. To examine possible roles of arterial baroreflex and vagal nerve activities in the effects of EA, we performed sinoaortic denervation and vagotomy. Approximately 20 min after the sinoaortic denervation and vagotomy, changes in AP, HR, CSNA, and RSNA in response to 10-Hz EA were examined.

Protocol 4. To confirm baroreflex-induced changes in sympathetic nerve activity, changes in CSNA and RSNA in response to an intravenous phenylephrine injection (5 μ g/kg) were examined before performing sinoaortic denervation and vagotomy. CSNA and

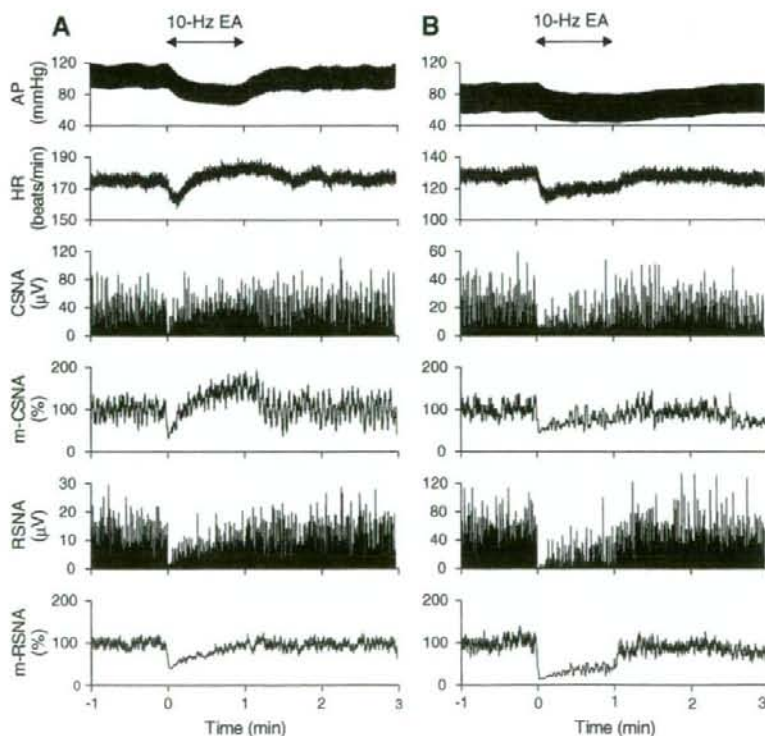


Fig. 1. Time series of arterial pressure (AP), heart rate (HR), cardiac sympathetic nerve activity (CSNA), 2-s moving averaged CSNA (m-CSNA), renal sympathetic nerve activity (RSNA), and 2-s moving averaged RSNA (m-RSNA) during 10-Hz electroacupuncture (EA) obtained from two different animals (see main text for details).

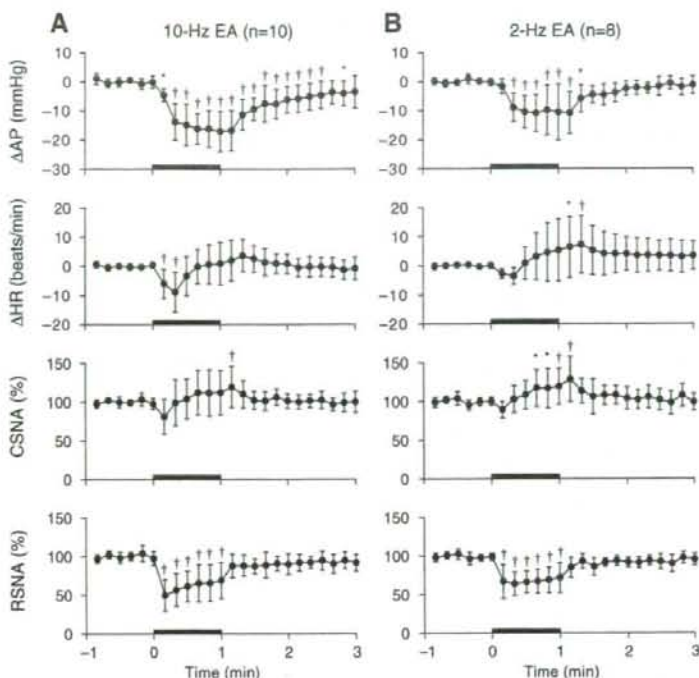


Fig. 2. Changes in arterial pressure (Δ AP), changes in heart rate (Δ HR), percent values of cardiac sympathetic nerve activity (CSNA), and percent values of renal sympathetic nerve activity (RSNA) during 10-Hz electroacupuncture (EA) (A) and 2-Hz EA (B) averaged for all trials. Values are the mean \pm SD. * $P < 0.05$ and † $P < 0.01$ from the first data point during the pre-EA baseline period.

RSNA were expected to be decreased by phenylephrine-induced hypertension.

2.4. Data analysis

Data were digitized by a 16-bit analog-to-digital converter (Contec, Japan) and stored at 200 Hz in a dedicated laboratory computer system. Because the absolute voltage of nerve activity varied among animals depending on the recording conditions, we normalized the nerve activity by a 1-min averaged value during the baseline condition before applying stimulation. The minimal inter-burst activity of the nerve signal was treated as the zero level. To examine changes in AP, HR, CSNA, and RSNA, we used 10-s averaged data. The data were analyzed using repeated-measures one-way analysis of variance (ANOVA) followed by Dunnett's test (Glantz, 2002). The first data point of the baseline condition was treated as the control. To analyze the correlation between changes in AP and CSNA or RSNA, that between changes in AP and changes in HR, and that between CSNA and RSNA, we performed a linear regression analysis between the two variables (Glantz, 2002). To analyze the correlation between changes in HR and CSNA or RSNA, we first fit the relationship to the following equation using a nonlinear least square fitting (a downhill simplex method) (Nelder and Mead, 1965).

$$y = \text{slope} \times \log_{10}(\text{offset} + x) + \text{intercept}$$

where x and y represent changes in HR and sympathetic nerve activity, respectively. After determining the optimal offset value for x , an ordinary linear regression analysis was performed between $[\log_{10}(\text{offset} + x)]$ and y to examine the significance of the slope. In all of the regression analyses, the correlation was considered significant when the slope was significantly different from zero. We used paired- t test

to examine the difference between the CSNA and RSNA during the time period of maximum AP elevation induced by phenylephrine in Protocol 4. To examine the difference in the initial HR response to 10-Hz EA between Protocols 1 and 3, we used unpaired- t test because the number of trials was different between Protocols 1 and 3. The differences were considered significant at $P < 0.05$.

3. Results

Typical recordings of 10-Hz EA obtained from two different cats are shown in Fig. 1. Horizontal arrows above the top panels indicate the period of EA. In one animal (Fig. 1A), AP was decreased by EA. HR decreased initially but increased from approximately 20 s after the onset of EA. As can be seen in the 2-s moving averaged signal (m-CSNA), CSNA exhibited changes similar to HR, i.e., it decreased at the onset of EA but gradually increased above the baseline level during the later portion of 1-min EA. RSNA and its 2-s moving averaged signal (m-RSNA) decreased at the onset of EA and gradually returned toward the baseline level. In another animal (Fig. 1B), both AP and HR were decreased by EA. Both CSNA and RSNA were also suppressed during EA, but the magnitude of suppression was greater in RSNA than in CSNA. Among the 5 animals, three showed the former type of AP and HR responses and remaining two showed the latter type. The type of AP and HR responses was consistent in each animal, i.e., the observed difference depended on the animal rather than the trial.

Fig. 2A summarizes changes in AP, HR, CSNA, and RSNA in response to 10-Hz EA. We performed EA trials in the left and right hind limbs in each animal and pooled data for 10 trials from 5 animals because there did not appear to be significant laterality in the effects of EA. The thick line on the abscissa in each panel indicates the period of EA. Baseline AP and HR values were 101 ± 17 mmHg and 161 ± 24 beats/min, respectively. AP was significantly decreased by EA and the decrease lasted over 1 min after

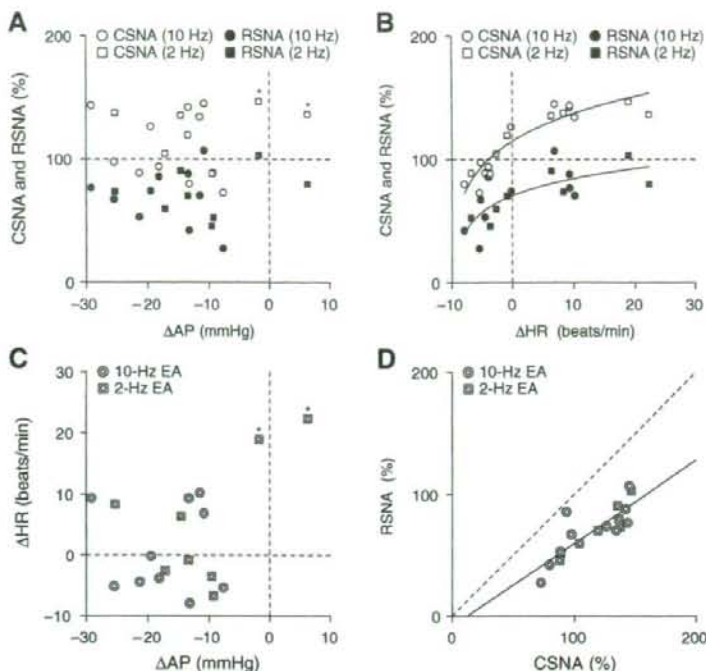


Fig. 3. Scatter plots of data obtained from the last 10 s of 1-min electroacupuncture (EA). A: Percent values of cardiac sympathetic nerve activity (CSNA) and renal sympathetic nerve activity (RSNA) plotted against changes in arterial pressure (Δ AP). Open and closed circles indicate CSNA and RSNA during 10-Hz EA, respectively. Open and closed squares indicate CSNA and RSNA during 2-Hz EA, respectively. Open squares with asterisks indicate data points where CSNA increased during EA even when AP did not decrease significantly or even increased. There was no significant relationship between changes in AP and CSNA ($r^2=0.0025$, $P=0.84$) or RSNA ($r^2=0.0039$, $P=0.81$). B: CSNA and RSNA plotted against changes in heart rate (Δ HR). Positive curvilinear relationships were observed between Δ HR and CSNA [$CSNA=83.0 \times \log_{10}(11.5 + \Delta HR) + 26.7$, $r^2=0.86$, $P<0.01$] and between Δ HR and RSNA [$RSNA=46.6 \times \log_{10}(10.1 + \Delta HR) + 23.6$, $r^2=0.56$, $P<0.01$]. C: Scatter plots of Δ HR versus Δ AP during 10-Hz EA (double circles) and 2-Hz EA (double squares). Except for the two data points with asterisks, there was no apparent relationship between changes in AP and those in HR ($r^2=0.17$, $P=0.094$ when the points with asterisk were included; $r^2=0.048$, $P=0.41$ when the points with asterisk were excluded). D: Scatter plots of RSNA versus CSNA during 10-Hz EA (double circles) and 2-Hz EA (double squares). There was a quasi-linear relationship between RSNA and CSNA ($RSNA=0.69 \times CSNA - 8.8$, $r^2=0.71$, $P<0.01$). The dashed line indicates the line of identity.

the cessation of EA. HR was significantly decreased in the first 20 s of EA but returned to the baseline level thereafter while EA continued. There was large variance in the CSNA response to EA among animals. Only the increase in CSNA after the cessation of EA was statistically significant. In contrast, RSNA was significantly decreased by EA during the entire period of EA.

Fig. 2B summarizes changes in AP, HR, CSNA, and RSNA in response to 2-Hz EA. We pooled data for 8 trials from 4 animals (left and right trials in each animal). Baseline AP and HR values were 98 ± 17 mmHg and 151 ± 20 beats/min, respectively. AP was decreased by EA, but the decrease was smaller and the duration of post-EA hypotension shorter than those observed in 10-Hz EA. HR increased with large variance during EA, and the increase was statistically significant after the cessation of EA. CSNA increased during the last 30 s of EA and remained increased for approximately 10 s after the cessation of EA. RSNA was decreased by EA during the period of EA, but the decrease appeared to be smaller than that observed with 10-Hz EA.

Fig. 3 illustrates scatter plots of data obtained during the last 10 s of EA. Because changes in AP nearly reached the steady state during the last 10 s of EA (Fig. 2A and B), we focused on these data. Open and closed circles in Fig. 3A and B indicate CSNA and RSNA data obtained from 10-Hz EA, respectively. Open and closed squares indicate CSNA and RSNA data obtained from 2-Hz EA, respectively. There was no apparent relationship between changes in AP and CSNA ($r^2=0.0025$, $P=0.84$) or RSNA ($r^2=0.0039$, $P=0.81$) by a linear regression analysis (Fig. 3A). In contrast, a positive curvilinear relationship was observed between changes in HR and CSNA [$CSNA=83.0 \times \log_{10}(11.5 + \Delta HR) + 26.7$, $r^2=0.86$, $P<0.01$] or RSNA

[$RSNA=46.6 \times \log_{10}(10.1 + \Delta HR) + 23.6$, $r^2=0.56$, $P<0.01$] (Fig. 3B). Double circles and squares in Fig. 3C and D indicate data obtained from 10-Hz EA and 2-Hz EA, respectively. In Fig. 3C, the two data points with asterisks indicate that 2-Hz EA increased HR by approximately 20 beats/min when changes in AP were close to zero or positive. However, except for the two data points, there was no apparent relationship between changes in AP and changes in HR ($r^2=0.17$, $P=0.094$ when the points with asterisk were included; $r^2=0.048$, $P=0.41$ when the points with asterisk were excluded). As indicated by Fig. 3A and B, the RSNA values were lower than the corresponding CSNA data (Fig. 3D), though CSNA and RSNA were both normalized to 100% during the baseline condition. A linear regression analysis revealed a significant positive correlation between CSNA and RSNA during the last 10 s of EA ($RSNA=0.69 \times CSNA - 8.8$, $r^2=0.71$, $P<0.01$).

As shown in Fig. 4A, there were no significant changes in AP, HR, CSNA, or RSNA during stimulation applied to a control point in the front of the right thigh. Baseline AP and HR values were 92 ± 15 mmHg and 158 ± 16 beats/min, respectively.

After sinoaortic denervation and vagotomy, baseline AP and HR values were 120 ± 25 mmHg and 184 ± 19 beats/min, respectively. As shown in Fig. 4B, 10-Hz EA decreased AP by approximately 30 mmHg. AP returned gradually to the pre-EA value after the cessation of EA. HR decreased slightly from 20 to 30 s and returned to the pre-EA baseline value thereafter. CSNA decreased only at the onset of EA. After the cessation of EA, CSNA exhibited a slight increase for approximately 20 s. RSNA decreased at the onset of EA. Although the magnitude of RSNA decrease became smaller with time, RSNA remained decreased during the period of EA.

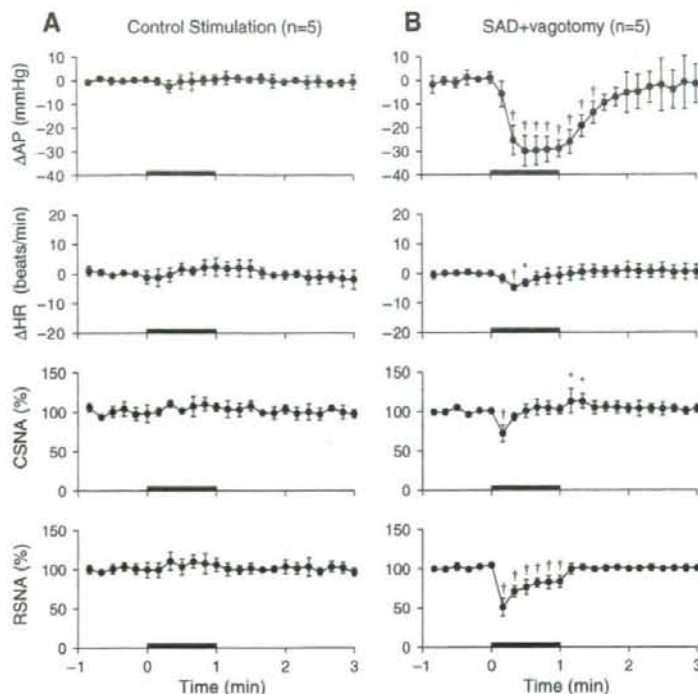


Fig. 4. Changes in arterial pressure (Δ AP), changes in heart rate (Δ HR), percent values of cardiac sympathetic nerve activity (CSNA), and percent values of renal sympathetic nerve activity (RSNA) during electrical stimulation at a nonspecific control point (A) and 10-Hz electroacupuncture (EA) after sinoaortic denervation (SAD) and vagotomy (B) averaged for all trials. Values are the mean \pm SD. * $P < 0.05$ and † $P < 0.01$ from the first data point during pre-EA baseline period.

Fig. 5A depicts changes in AP, HR, CSNA, and RSNA induced by intravenous bolus injection of phenylephrine (5 μ g/kg). The data were obtained before sinoaortic denervation and vagotomy. Baseline AP and HR values were 98 ± 24 mmHg and 163 ± 30 beats/min, respectively. As expected, phenylephrine increased AP but decreased HR. Both CSNA and RSNA were decreased by phenylephrine injection. The suppression of CSNA persisted longer than that of RSNA. There was no significant correlation between CSNA and RSNA during the baseline condition immediately before the administration of phenylephrine (Fig. 5B, white circles, $r^2 = 0.32$, $P = 0.32$). When CSNA and RSNA were compared during the time period of phenylephrine-induced maximum AP elevation, there was no significant correlation either (Fig. 5B, filled circles, $r^2 = 0.0003$, $P = 0.98$).

4. Discussion

We have demonstrated that CSNA and RSNA responded differentially to EA applied to a hind limb in pentobarbital-anesthetized cats. Although the CSNA and RSNA responses were discordant, we found that CSNA and RSNA attained a new linear relationship during the last 10 s of EA (Fig. 3D), regardless of the stimulus frequency of EA.

4.1. Effects of EA on CSNA and RSNA

The neural mechanisms underlying hemodynamic responses to acupuncture are not fully understood. Recently, Uchida et al. (2007) demonstrated that manual acupuncture-like stimulation of a hind limb decreased CSNA and HR in pentobarbital-anesthetized rats. Their results complement the study by Ohsawa et al. (1995) showing that manual acupuncture-like stimulation decreased RSNA and AP. Although these results suggest that manual acupuncture-like stimulation causes systemic sympathoinhibition, we noted that HR did not necessarily de-

crease even when EA produced hypotensive effects in pentobarbital-anesthetized cats (Figs. 1A and 2A and B). Simultaneous recordings of CSNA and RSNA in the present study clearly supported the hypothesis that EA evoked regional differences among sympathetic nerve activities. Fig. 1A is a typical case in which CSNA increased without an associated increase in RSNA during the later portion of EA. In Protocol 2, no significant changes were observed (Fig. 4A), suggesting that hemodynamic and sympathetic nerve activity responses observed in Protocol 1 were not nonspecific responses to electrical stimulation. This does not mean, however, the point below the knee joint just lateral to the tibia (corresponding to an ST36 acupoint in humans) is the only specific point to produce cardiovascular responses. For instance, EA at the forelimb (corresponding to a PC6 acupoint in humans) exerts the cardiovascular effects in rats (Lujan et al., 2007).

Averaged data for 10-Hz EA (Fig. 2A) revealed a discrepancy between the CSNA and RSNA responses to EA. Both sympathoinhibition and sympathoexcitation appear to have occurred in CSNA during EA. We suspected that strong electrical stimulation might have caused nociceptive sympathoexcitatory responses in CSNA. However, reducing the stimulus frequency from 10 to 2 Hz resulted in a more pronounced excitatory response in CSNA during the later period of 1-min EA (Fig. 2B), suggesting that the increase in CSNA during EA was not a nociceptive response. Another factor that should be taken into account is effects of anesthesia. Matsukawa et al. (Matsukawa et al., 1993) demonstrated that sympathoinhibition induced by acute intravenous pentobarbital administration was larger and lasted longer in the case of CSNA than in that of RSNA in cats. The sympathoinhibitory response to EA may be easily observed when the baseline sympathetic tone is high. Because baseline sympathetic tone was probably lower in CSNA than in RSNA due to the pentobarbital anesthesia, the sympathoinhibitory response in CSNA might have been masked or hard to observe.

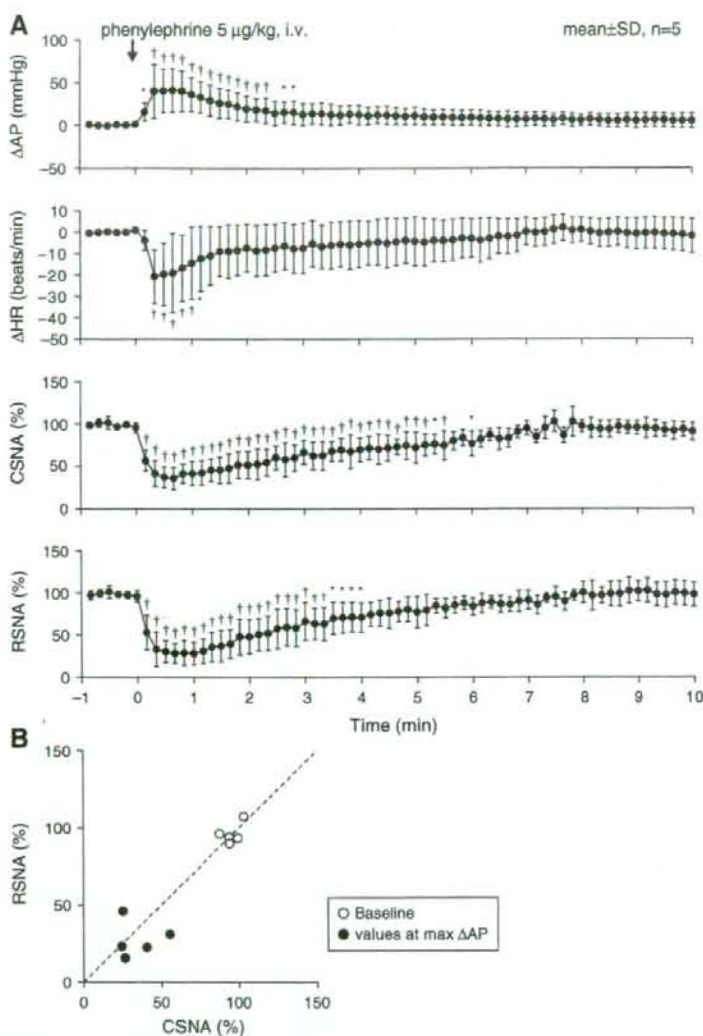


Fig. 5. A: Changes in arterial pressure (ΔAP), changes in heart rate (ΔHR), percent values of cardiac sympathetic nerve activity (CSNA), and percent values of renal sympathetic nerve activity (RSNA) during intravenous bolus injection of phenylephrine (5 $\mu\text{g}/\text{kg}$). Values are the mean \pm SD. * $P < 0.05$ and † $P < 0.01$ from the first data point during the baseline period. B: Scatter plots between CSNA and RSNA during the baseline condition immediately before the administration of phenylephrine (white circles) and those during the time period of phenylephrine-induced maximum AP elevation (filled circles). There was no significant correlation between CSNA and RSNA. The dashed line indicates the line of identity.

Although we measured left CSNA near the ventral ansa of the left stellate ganglion, there are several connections between the vagal and sympathetic nerves to form the cardiopulmonary nerves (Armour and Hopkins, 1984). Because we did not cut the vagi at the neck in Protocols 1 and 2, possibility of vagal contamination in the CSNA recording cannot be ruled out. However, because phenylephrine-induced hypertension that can increase vagal efferent activity (Kawada et al., 2001) attenuated CSNA to a similar degree to RSNA during the time period of maximum AP elevation ($38.5 \pm 13.4\%$ vs. $28.6 \pm 10.5\%$, $P = 0.32$ by paired- t test, Fig. 5A), the effect of vagal contamination might have been a limited one.

4.2. Mechanistic considerations

In the present experimental settings, CSNA and RSNA exhibited decreasing responses to arterial baroreflex activation as demonstrated in previous studies (Fig. 5) (Minisi et al., 1989; Ninomiya et al., 1971),

confirming that what we measured as CSNA and RSNA represented efferent sympathetic nerve activities. Because EA caused hypotension, it could exert sympathoexcitatory effects through the arterial baroreflex in Protocol 1. If the baroreflex-mediated sympathoexcitatory effect is stronger for CSNA than for RSNA, this may account for the discrepancy between the CSNA and RSNA responses. However, in some trials, CSNA was increased even when AP did not decrease sizably or was even increased (Fig. 3A, open squares with asterisks), suggesting that the baroreflex-mediated sympathoexcitatory effect cannot explain the increase in CSNA. Actually, the discrepancy between the CSNA and RSNA responses to 10-Hz EA persisted after sinoaortic denervation and vagotomy (Fig. 4B). Therefore, CSNA might have been activated in the later period of EA via mechanisms other than baroreflexes. This interpretation is in line with the conclusion by Sato et al. (1981) that variable changes in HR in response to somatic afferent stimulation were not an indirect consequence of preceding changes in blood pressure.

Although electrical stimulation of groups I and II muscle nerves of fore and hind limbs was not effective in changing HR (McCloskey and Mitchell, 1972; Sato et al., 1981), additional stimulation of group III nerves induced either tachycardia or bradycardia in anesthetized cats (Khayutin et al., 1986; Sato et al., 1981). Further, additional stimulation of group IV muscle nerves of a hind limb always produced tachycardia (Johansson, 1962; Tibes, 1977), with an optimal frequency between 6 and 15 Hz (Sato et al., 1981). In the present study, activation of group IV muscle nerves unlikely explain the tachycardiac response, since reducing the stimulus frequency from 10 to 2 Hz did not attenuate the tachycardiac response. Although Sato et al. (1981) concluded that whether group III muscle afferent stimulation induces tachycardia or bradycardia was difficult to predict, we found that there was a quasi-linear relationship between RSNA and CSNA during the last 10 s of 1-min EA, regardless of the stimulus frequency (Fig. 3D). When the sympathoinhibition assessed by RSNA was strong enough, CSNA decreased during EA. When the sympathoinhibition assessed by RSNA was weak, CSNA increased.

4.3. Limitations

Several limitations need to be addressed. First, we performed experiments under pentobarbital anesthesia. Our results might have differed had we used different anesthesia or performed the experiments in conscious animals. However, Sato et al. (1981) used chloralose and urethane anesthesia and reported divergence of HR responses induced by group III muscle fiber afferent stimulation. Therefore, the differences between CSNA and RSNA might not be explained by type of anesthesia alone.

Second, we measured only CSNA and RSNA. Changes in AP did not correlate with CSNA or RSNA (Fig. 3A), suggesting that the AP response to EA was not explained by changes in CSNA or RSNA. The abdominal vascular bed plays a significant role in the arterial blood pressure control (Rowell, 1974). Further studies such as that recording splanchnic nerve activity are needed to elucidate the total picture of the sympathetic mechanism for the AP response to EA.

Third, we did not perform vagotomy independently of sinoaortic denervation. Accordingly, the contribution of vagal nerve activity to the HR response was not identified. Comparing Figs. 2A and 4B, the initial drop in HR was much clearer before sinoaortic denervation and vagotomy ($P=0.025$ during the first 10 s after EA initiation by unpaired-*t* test) despite the similar profile of CSNA response to EA. Therefore, the vagal nerve activity might have contributed to the initial drop in HR in response to EA.

4.4. Conclusion

We demonstrated that EA evoked regional differences between CSNA and RSNA in pentobarbital-anesthetized cats. The differences persisted after sinoaortic denervation and vagotomy, suggesting the baroreflex-mediated sympathoexcitatory mechanisms alone cannot explain the discrepancy between CSNA and RSNA responses during EA. Although the responses were discordant, there was a linear relationship that persisted between CSNA and RSNA during the last 10 s of 1-min EA, suggesting that EA changes the relationship between CSNA and RSNA.

Acknowledgments

This study was supported by a "Health and Labour Sciences Research Grant for Research on Advanced Medical Technology", "Health and Labour Sciences Research Grant for Research on Medical Devices for Analyzing, Supporting, and Substituting the Function of the Human Body", and a "Health and Labour Sciences Research Grant (H18-Iryo-Ippan-023) (H18-Nano-Ippan-003)", from the Ministry of Health, Labour, and Welfare of Japan, the "Industrial Technology Research

Grant Program" of the New Energy and Industrial Technology Development Organization of Japan.

References

- Armour, J.A., Hopkins, D.A., 1984. Anatomy of the extrinsic efferent autonomic nerves and ganglia innervating the mammalian heart. In: Randall, W.C. (Ed.), *Nervous Control of Cardiovascular Function*. Oxford Univ. Press, New York, pp. 20–45.
- DiBona, G.F., 2005. Physiology in perspective: the wisdom of the body. Neural control of the kidney. *Am. J. Physiol., Regul. Integr. Comp. Physiol.* 289 (3), R633–641.
- Glantz, S.A., 2002. *Primer of Biostatistics*, 5th ed. McGraw-Hill, New York.
- Johansson, B., 1962. Circulatory responses to stimulation of somatic afferents with special reference to depressor effects from muscle nerves. *Acta Physiol. Scand., Suppl.* 198, 1–91.
- Kawada, T., Yamazaki, T., Akiyama, T., Shishido, T., Inagaki, M., Uemura, K., Miyamoto, T., Sugimachi, M., Takaki, H., Sunagawa, K., 2001. In vivo assessment of acetylcholine-releasing function at cardiac vagal nerve terminals. *Am. J. Physiol. Heart Circ. Physiol.* 281 (1), H139–145.
- Kawada, T., Uemura, K., Kashihara, K., Jin, Y., Li, M., Zheng, C., Sugimachi, M., Sunagawa, K., 2003. Uniformity in dynamic baroreflex regulation of left and right cardiac sympathetic nerve activities. *Am. J. Physiol., Regul. Integr. Comp. Physiol.* 284 (6), R1506–1512.
- Khayutin, V.M., Lukoshkova, E.V., Gailans, J.B., 1986. Somatic depressor reflexes: results of specific 'depressor' afferents' excitation or an epiphenomenon of general anesthesia and certain decerebrations? *J. Auton. Nerv. Syst.* 16 (1), 35–60.
- Kimura, A., Sato, A., 1997. Somatic regulation of autonomic functions in anesthetized animals—neural mechanisms of physical therapy including acupuncture. *Jpn. J. Vet. Res.* 45 (3), 137–145.
- Kline, R.L., Yeung, K.Y., Calaresu, F.R., 1978. Role of somatic nerves in the cardiovascular responses to stimulation of an acupuncture point in anesthetized rabbits. *Exp. Neurol.* 61 (3), 561–570.
- Kobayashi, S., Noguchi, E., Ohsawa, H., Sato, Y., Nishijo, K., 1998. Experimental research on the reflex decrease of heart rate elicited by acupuncture stimulation in anesthetized rats (in Japanese). *Jpn. Acupunct. Moxib.* 48, 120–129.
- Ku, Y.H., Zou, C.J., 1993. Tinggong (SI 19), a novel acupoint for 2 Hz electroacupuncture-induced depressor response. *Acupunct. Electrother. Res.* 18 (2), 89–96.
- Lee, H.S., Kim, J.Y., 1994. Effects of acupuncture on blood pressure and plasma renin activity in two-kidney one clip Goldblatt hypertensive rats. *Am. J. Chin. Med.* 22 (3–4), 215–219.
- Lin, M.C., Nahin, R., Gershwin, M.E., Longhurst, J.C., Wu, K.K., 2001. State of complementary and alternative medicine in cardiovascular, lung, and blood research: executive summary of a workshop. *Circulation* 103 (16), 2038–2041.
- Lujan, H.L., Kramer, V.J., DiCarlo, S.E., 2007. Electroacupuncture decreases the susceptibility to ventricular tachycardia in conscious rats by reducing cardiac metabolic demand. *Am. J. Physiol. Heart Circ. Physiol.* 292 (5), H2550–H2555.
- Matsukawa, K., Ninomiya, L., Nishiura, N., 1993. Effects of anesthesia on cardiac and renal sympathetic nerve activities and plasma catecholamines. *Am. J. Physiol.* 265 (4 Pt 2), R792–R797.
- McCloskey, D.J., Mitchell, J.H., 1972. Reflex cardiovascular and respiratory responses originating in exercising muscle. *J. Physiol.* 224 (1), 173–186.
- Minisi, A.J., Dibner-Dunlap, M., Thames, M.D., 1989. Vagal cardiopulmonary baroreflex activation during phenylephrine infusion. *Am. J. Physiol.* 257 (5 Pt 2), R1147–R1153.
- Neider, J.A., Mead, R., 1965. A simplex method for function minimization. *Comput. J.* 7, 308–313.
- Ninomiya, L., Nisamaru, N., Irisawa, H., 1971. Sympathetic nerve activity to the spleen, kidney, and heart in response to baroreceptor input. *Am. J. Physiol.* 221 (5), 1346–1351.
- Ohsawa, H., Okada, K., Nishijo, K., Sato, Y., 1995. Neural mechanism of depressor responses of arterial pressure elicited by acupuncture-like stimulation to a hindlimb in anesthetized rats. *J. Auton. Nerv. Syst.* 51 (1), 27–35.
- Rowell, L.B., 1974. Human cardiovascular adjustments to exercise and thermal stress. *Physiol. Rev.* 54 (1), 75–159.
- Sato, A., Sato, Y., Schmidt, R.F., 1981. Heart rate changes reflecting modifications of efferent cardiac sympathetic outflow by cutaneous and muscle afferent volleys. *J. Auton. Nerv. Syst.* 4 (3), 231–247.
- Sato, A., Sato, Y., Suzuki, A., Uchida, S., 1994. Reflex modulation of gastric and vesical function by acupuncture-like stimulation in anesthetized rats. *Biomed. Res.* 15, 59–65.
- Sato, A., Sato, Y., Uchida, S., 2002. Reflex modulation of visceral functions by acupuncture-like stimulation in anesthetized rats. *Int. Congr. Ser.* 1238, 111–123.
- Tibes, U., 1977. Reflex inputs to the cardiovascular and respiratory centers from dynamically working canine muscles. Some evidence for involvement of group III or IV nerve fibers. *Circ. Res.* 41 (3), 332–341.
- Uchida, S., Shimura, M., Ohsawa, H., Suzuki, A., 2007. Neural mechanism of bradycardiac responses elicited by acupuncture-like stimulation to a hind limb in anesthetized rats. *J. Physiol. Sci.* 57 (6), 377–382.
- Yasunaga, K., Nosaka, S., 1979. Cardiac sympathetic nerves in rats: anatomical and functional features. *Jpn. J. Physiol.* 29 (6), 691–705.
- Zhou, W., Fu, L.W., Tjen, A.L.S.C., Li, P., Longhurst, J.C., 2005. Afferent mechanisms underlying stimulation modality-related modulation of acupuncture-related cardiovascular responses. *J. Appl. Physiol.* 98 (3), 872–880.

Accentuated Antagonism in Vagal Heart Rate Control Mediated through Muscarinic Potassium Channels

Masaki MIZUNO¹, Atsunori KAMIYA¹, Toru KAWADA¹, Tadayoshi MIYAMOTO²,
Shuji SHIMIZU^{1,3}, Toshiaki SHISHIDO¹, and Masaru SUGIMACHI¹

¹Department of Cardiovascular Dynamics, Advanced Medical Engineering Center, National Cardiovascular Center Research Institute, Osaka, Japan; ²Department of Physical Therapy, Faculty of Health Sciences, Morinomiyama University of Medical Sciences, Osaka, Japan; and ³Japan Association for the Advancement of Medical Equipment, Tokyo, Japan

Abstract: Although muscarinic K⁺ (K_{ACH}) channels contribute to a rapid heart rate (HR) response to vagal stimulation, whether background sympathetic tone affects the HR control via the K_{ACH} channels remains to be elucidated. In seven anesthetized rabbits with sinoaortic denervation and vagotomy, we estimated the dynamic transfer function of the HR response by using random binary vagal stimulation (0–10 Hz). Tertiapin, a selective K_{ACH} channel blocker, decreased the dynamic gain (to 2.3 ± 0.9 beats·min⁻¹·Hz⁻¹, from 4.6 ± 1.1 , $P < 0.01$, mean \pm SD) and the corner frequency (to 0.05 ± 0.01 Hz, from 0.26 ± 0.04 , $P < 0.01$). Under 5 Hz tonic cardiac sympathetic stimulation (CSS), tertiapin decreased the dynamic gain (to 3.6 ± 1.0 beats·min⁻¹·Hz⁻¹,

from 7.3 ± 1.1 , $P < 0.01$) and the corner frequency (to 0.06 ± 0.02 Hz, from 0.23 ± 0.06 , $P < 0.01$). Two-way analysis of variance indicated significant interaction between the tertiapin and CSS effects on the dynamic gain. In contrast, no significant interactions were observed between the tertiapin and CSS effects on the corner frequency and the lag time. In conclusion, although a cyclic AMP-dependent mechanism has been well established, an accentuated antagonism also occurred in the direct effect of ACh via the K_{ACH} channels. The rapidity of the HR response obtained by the K_{ACH} channel pathway was robust during the accentuated antagonism.

Key words: systems analysis, transfer function, muscarinic receptor, sympathovagal interaction, accentuated antagonism, rabbit.

Vagal control of heart rate (HR) is mediated by ACh, which activates M₂ muscarinic receptors and heterotrimeric G_i and/or G_o proteins in cardiac myocytes [1]. The actions of ACh are determined by the G_i protein subunits. The α subunits of the G_i proteins inhibit adenylyl cyclase and decrease HR by counteracting the sympathetic effects [2], whereas $\beta\gamma$ subunits activate inwardly rectifying muscarinic K⁺ (K_{ACH}) channels and decrease HR by hyperpolarizing the maximum diastolic potential in the sinus node cells [3–5]. Hereafter in the present paper, we refer to the former action as the indirect action of ACh and the latter action as the direct action of ACh. In a previous paper, we demonstrated that a selective K_{ACH} channel blocker tertiapin decreased and slowed the HR response to dynamic vagal stimulation, suggesting that the K_{ACH} channels contribute to a rapid HR response to vagal stimulation [6]. However, whether background sympathetic tone affects HR control via the K_{ACH} channels remains to be elucidated. Because pathophysiological conditions such as chronic heart failure [7], hypertension [8], and obesity [9] often display increased sympathetic nerve

activity, it would be important to quantify the effects of background sympathetic tone on the HR response via the K_{ACH} channels for a better understanding of the vagal HR control in such disease states.

We made two hypotheses regarding sympathetic effects on vagal HR control via the K_{ACH} channels. With respect to the speed of HR regulation, the indirect action of ACh relies on slower changes in intracellular cyclic AMP levels [10, 11]. In contrast, the direct action of ACh utilizes the faster membrane-delimited mechanisms of K_{ACH} channels and is believed to be independent of sympathetic control [12]. Accordingly, we first hypothesized that background sympathetic tone would not affect the *rapidity* of HR control provided by the K_{ACH} channel pathway. With respect to the magnitude of HR regulation, complex sympathovagal interactions can occur in autonomic HR control. Levy [13] termed the phenomenon that background sympathetic tone augmented vagal HR control “an accentuated antagonism.” Kawada *et al.* [14] demonstrated that sympathovagal interaction bidirectionally increased the dynamic gain of HR control, even

Received on Jul 31, 2008; accepted on Sep 5, 2008; released online on Oct 10, 2008; doi:10.2170/physiolsci.RP011508

Correspondence should be addressed to: Masaki Mizuno, Department of Cardiovascular Dynamics, Advanced Medical Engineering Center, National Cardiovascular Center Research Institute, 5-7-1 Fujishirodai, Suita, Osaka, 565-8565 Japan. Tel: +81-6-6833-5012 (Ext. 2427), Fax: +81-6-6835-5403, E-mail: m-mizuno@ri.ncvc.go.jp

though the sympathetic and vagal systems affected mean HR antagonistically. Therefore we then hypothesized that background sympathetic tone would augment the magnitude of the HR response to vagal stimulation via K_{ACh} channels.

To test the above-mentioned hypotheses, we examined the dynamic and static transfer characteristics of the HR response to vagal stimulation using a selective K_{ACh} channel blocker tertiapin and concomitant cardiac sympathetic stimulation (CSS). Observation of significant interaction between tertiapin and CSS effects might allow us to deduce that background sympathetic tone influences the direct action of ACh via K_{ACh} channels.

MATERIALS AND METHODS

Surgical preparations. Animal care was consistent with "Guiding Principles for the Care and Use of Animals in the Field of Physiological Sciences" of the Physiological Society of Japan. All protocols were reviewed and approved by the Animal Subjects Committee of the National Cardiovascular Center. Seven Japanese white rabbits (2.7–3.2 kg body wt) were anesthetized using a mixture of urethane (250 mg/ml) and α -chloralose (40 mg/ml): an initial bolus dose of 2 ml/kg and a maintenance dose of 0.5 ml·kg⁻¹·h⁻¹. The rabbits were intubated and mechanically ventilated with oxygen-enriched room air. Arterial pressure (AP) was measured by a micromanometer (SPC-330A, Millar Instruments, Houston, TX, USA) inserted into the right femoral artery and advanced to the thoracic aorta. HR was measured with a cardiometer (model N4778, San-ei, Tokyo, Japan). A double-lumen catheter was introduced into the right femoral vein for continuous anesthetic and drug administration. Sinoaortic denervation was performed bilaterally to minimize changes in sympathetic efferent nerve activity via arterial baroreflexes. The main branches of the cardiac postganglionic sympathetic nerves were sectioned bilaterally through a midline thoracotomy. A pair of bipolar platinum electrodes was attached to the cardiac end of the sectioned right inferior cardiac sympathetic postganglionic nerve for tonic cardiac sympathetic nerve stimulation [15]. The vagi were sectioned bilaterally at the neck. Another pair of bipolar electrodes was attached to the cardiac end of the sectioned right vagus for vagal stimulation. Immersion of the stimulation electrodes and nerves in a mixture of white petroleum jelly (Vaseline) and liquid paraffin prevented the nerves from drying and also provided insulation. Body temperature was maintained at 38°C with a heating pad throughout the experiment.

Experimental protocols. The pulse duration of nerve stimulation was set at 2 ms. The stimulation amplitude of the right vagus was first adjusted in each animal to yield an HR decrease of ~50 beats/min at 10 Hz constant stimulation (1.6–6.0 V, 3.2 ± 1.7 V, mean \pm SD) and fixed.

The stimulation amplitude of the right cardiac sympathetic nerve was also adjusted in each animal to yield an HR increase of ~50 beats/min at 5 Hz constant stimulation (1.5–3.5 V, 2.2 ± 0.8 V) and fixed. Approximately 1 h elapsed after the completion of surgical preparation until stable hemodynamics were attained.

Dynamic protocol ($n = 7$). For an estimation of the dynamic transfer characteristics from vagal stimulation to the HR response, the right vagus was stimulated by a frequency-modulated pulse train for 10 min. The stimulation frequency was switched every 500 ms at either 0 or 10 Hz according to a binary white-noise signal. The power spectrum of the stimulation signal was reasonably constant up to 1 Hz. The transfer function was estimated up to 1 Hz because the reliability of estimation decreased as a result of the diminution of input power above this frequency. The selected frequency range spanned the frequency range of physiological interest sufficiently with respect to the dynamic vagal control of HR in rabbits.

Static protocol ($n = 5$). For an estimation of the static transfer characteristics between vagal stimulation and HR response, stepwise vagal stimulation was performed. Vagal stimulation frequency was increased to 20 Hz, from 5, in 5 Hz increments. Each frequency step was maintained for 60 s.

Pharmacological intervention. We used a selective K_{ACh} channel blocker tertiapin (Peptide Institute, Inc., Osaka, Japan) to block the direct action of ACh in vagal HR control. The dynamic and static characteristics of the heart rate response to vagal stimulation were estimated with and without CSS. After the tertiapin-free data were obtained, a bolus dose (30 nmol/kg iv) of tertiapin was administered. Fifteen min thereafter, the dynamic and static characteristics were estimated again, with and without CSS. The tertiapin-free data were obtained first in all animals because the long-lasting (>2 h) effects of tertiapin did not permit the acquisition of tertiapin-free data after the tertiapin administration. The order of dynamic and static protocols and the order of CSS application were randomly assigned in different animals. An intervening interval of more than 5 min was allowed between the dynamic and static protocols so that AP and HR returned their prestimulation values.

Data analysis. A 12-bit analog-to-digital converter was used to digitize the AP and HR recordings at 200 Hz, and the data were stored on the hard disk of a dedicated laboratory computer system. The dynamic transfer function from binary white-noise vagal stimulation to the HR response was estimated as follows. Input-output data pairs of the vagal stimulation frequency and HR were resampled at 10 Hz; then data pairs were partitioned into eight 50%-overlapping segments, each consisting of 1,024 data points. For each segment, the linear trend was subtracted and a Hanning window applied. A fast Fourier transform was then performed to obtain the frequency